The Journal of Engineering Research (TJER) Vol. 13, No. 1 (2016) 22-32

Effect of Sediment Density on the Bed Topography in a Channel Bend Using Numerical Modeling

M. Vaghefi*, a, Y. Safarpoor and S.S. Hashemi

Civil Engineering Department, Persian Gulf University, Bushehr, Iran

Received 25 February 2015; Accepted 13 August 2015

Abstract: In this paper, the bed topography of a channel at a 90-degree bend was studied at the T-shaped spur dike installed at the middle of the outer bank. Numerical analyses were performed with the Sediment Simulation in Intakes with Multiblock Option (SSIIM) model. Three relative curvatures (*R/B* = 2, 3, and 4) related to the three sediment densities (*P* = 2.35, 2.5, and 2.65) were modeled in nine cases and the effects of sediment density on the bed scour patterns were studied. It was observed that the maximum amount of scour occurred near the head of the dike wing at the dike's upstream, and the maximum amount of sedimentation occurred at the inner bank of the bend exit. By increasing the sediment density when *R/B* = 4, the maximum scour and sedimentation decreased to 27.41% and 46.15%, respectively. When *R/B* = 3, the maximum scour and sedimentation decreased to 25.93% and 23.91%, respectively. When *R/B* = 2, the maximum scour and sedimentation decreased to 25.98% and 10%, respectively.

Keywords: SSIIM model, T-shaped spur dike channel bend, Sediment density, Relative curvature.

تأثير كثافة الرُسابة على الطوبوغرافية الطبقية في منحنى القناة باستخدام نموذج عددي

فاكهفي محمد[أ], سفربور ياسر ، وهاشمي سيد شاكر

الملخص: في هذه الورقة تم دراسة الطبوغرافية الطبقية لقناة لها ٩٠ درجة من الانحناء. تم تركيب سد مسنن على شكل حرف تائية في منتصف المقعد الخارجي. أجريت التحليلات العددية مع نموذج SSIIM. تم نمذجة ثلاثة انحناءات نسبية (ر/ب=٢، ٣، ٤) متعلقة بثلاث كثافات للرسابة (2.35, 2.5, 2.65) في ٩ حالات، ودراسة تأثيرات كثافة الرُسابة على أنماط التنظيف الطبقية. لوحظ أن أكبر قدر ممكن من التنظيف يحدث بالقرب من مقدمة جناح السد، وأكبر قدر ممكن من الترسيب يحدث في المقعد الداخلي لانحناء الخروج. عن طريق زيادة كثافة الرُسابة عندما تكون نسبة ر/ب=٤، وجد الحد الأقصى للتنظيف والترسيب ينخفض إلى ٢٧,٤١٪ و٤٦,١٥٪ على التوالي؛ وعندما تكون نسبة ر/ب=٣، وجد الحد الأقصى للتنظيف والترسيب ينخفض إلى ٢٥,٩٣٪ و٢٣,٩١٪ على التوالي؛ وعندما تكون نسبة ر/ب=٢، وجد الحد الأقصى للتنظيف والترسيب ينخفض إلى ٢٥,٩٨٪ و١٠٪ على التوالي.

الكلمات المفتاحية: نموذج SSIIM، حفز السد على شكل ت، منحنى القناة، كثافة الرُسابة. الانحناء النسبي.

* Corresponding author's e-mail: Vaghefi@pgu.ac.ir

1. Introduction

One of the methods employed for river training is the use of spur dike structures. Spur dikes divert the mainstream and protect river banks from erosion and have been studied for many years by researchers. Numerical model simulations are usually more cost-effective and faster than physical model studies and have no inherent limitations on spatial extent (Hua *et al*. 2006).

To study the curved channels, it is necessary to first check the flow pattern affected by cross-flow and secondary flow. Shukry (1949) presented an equation for calculating the power of secondary flow in channel bends. Nouh and Townsend (1979) determined that the secondary flow after leaving the bend not only is lost, but continues a straight distance downstream. Gill (1972), by changing the radius of curve, depth of flow and diameter of particles in the direct and bend channels showed that the distance between spur dikes is dependent on the radius of the curve. Da Silva and Yalin (1997) discussed the locations of the sediments and erosion holes in two mild and sharp meander bends. Lian *et al.* (1999) found that the secondary flow in a 180-degree bend is stronger than that in a 90-degree one. The curvature of the flow in river bends leads to secondary flow normal to the main flow's direction. In a river bend, a large secondary flow cell develops, covering most of the cross-section. Moreover, in river bends with steep outer banks, a much weaker second, counter rotating, secondary flow cell appears along the upper part of the outside river bank (Booij 2002). One of the consequences arising from the installation of a spur dike is the creation of scour around the spur dike bed which is caused by a change in the flow pattern of the channel. Elawady *et al*. (2001) concluded that the scouring around a submerged spur dike is affected by the submergence and opening ratios of a channel. A greater opening ratio leads to a reduction in scour and the erosion of downstream banks rarely occurs.

One type of spur dike is a T-shaped spur dike. Because of the cross section at the tip of the spur dike (the dike wing), it has a different impact relative to direct and normal spur dikes, and it has a unique effect on the pattern of flow and the scour. This effect occurs because the longer longitudinal section of the channel is blocked. In a T-shaped spur dike, the dike wing reduces the scouring in the bed of a dike web.

The effects of the dike and Froude number on the scour around a T-shaped spur dike in a 90-degree bend was examined by Ghodsian and Vaghefi (2009). It was found that the dimensions of the scour hole increased as a result of an increase in the length of the spur dike. Additionally, it was determined that by increasing the Froude number and length of the spur dike, the amount of scour increases. For bank protection purposes, the spacing-to-length ratio of the spur dikes is limited to a maximum value of six due to the characteristics of the vortex system (Azinfar 2010).

Several numerical models have been used to calculate flow patterns and sediment but in this study, the SSIIM numerical model has been employed because of its ability to analyze the flow and scour patterns in the channel with complex geometry. An experimental and numerical simulation of flow using the Sediment Simulation in Intakes with Multiblock Option (SSIIM) model showed that the SSIIM model could accurately simulate the flow pattern in 90 degree bends (Abhari *et al*. 2010). In meander bends, the velocity distribution and angle of attack are indicative of secondary currents associated with channel curvature (Sclafani *et al*. 2012). Vaghefi *et al.* (2014) studied the effect of the T-shaped spur dike submergence ratio on the water surface profile using the SSIIM model. They showed that the flow velocity over the spur dike crest level will be greater with the increase of T-shaped spur dike submergence. Vaghefi *et al.* (2015) calibrated the SSIIM numerical model based on the experimental model in a channel bend; therefore, in this study the SSIIM model was used. There has been no thorough investigation of the effect of changes in sediment density on a river bed's curved channels or a comparison of them in different relative curvatures. What makes this study important is the numerical study of scour pattern in channel bed under the influence of a T-shaped dike. The types of sediments in a river bed in order of density, diameter, and fall velocity affect the calculations of sediment transport; therefore, in this study, the variations of the bed topography were evaluated at the channel bend with three different relative curvatures due to changes in sediment density.

2. Materials and Methods

2.1 Numerical Model

The SSIIM numerical model addresses the Navier-Stokes equations with the k-ε model on a three-dimensional (3D) general non-orthogonal grid. In SSIIM, the Navier-Stokes equations for turbulent flow in a general 3D geometry are solved to obtain water velocity. The Navier-Stokes equations for non-compressible and flow with constant density can be expressed as follows:

$$\frac{\partial U_i}{\partial t}+U_j\frac{\partial U_i}{\partial x_i}=\frac{1}{\rho}\frac{\partial}{\partial x_i}\left(-P\delta_{ij}-\overline{\rho U_i U_j}\right) \quad (1)$$

where x_1, x_2, and x_3 are distances and U_1, U_2, and U_3 are the velocities in three directions. P is pressure and δ_{ij} is the Kronecker delta that is equal to unity for i = j, and zero otherwise. The first term on the left side of the equation is the transient term while the next term is the convective term. The first term on the right-hand side is the pressure term while the second term on the right side of equation is the Reynolds stress term and, to evaluate this term, k-ε turbulence model is used. The semi-implicit method for pressure-linked equations (SIMPLE) was used to compute the pressure term. The effect of the density variations on the water flow field is taken into account by introducing a modified eddy viscosity. The eddy viscosity from the k-ε model is multiplied with a factor, taking into account the velocity and concentration gradients. Sediment transport is traditionally divided into bed and suspended loads. For suspended load, Van Rijn (1987) developed a formula for the equilibrium sediment concentration, C_{bed}, close to the bed (Eqn. 2). In addition to the suspended load, the bed load, q_b, can be calculated. In (Eqn. 3), Van Rijn's formula for bed load is used (2007).

$$C_{bed}=0.015\frac{d^{0.3}}{a}\frac{\left[\frac{\tau-\tau_c}{\tau_c}\right]^{1.5}}{\left[\frac{(\rho s-\rho w)g}{\rho w \upsilon^2}\right]^{0.1}} \quad (2)$$

$$\frac{q_b}{D_{50}^{1.5}\sqrt{\left(\frac{\rho s-\rho w}{\rho w}\right)g}}=0.053\frac{\left[\frac{\tau-\tau c}{\tau c}\right]^{1.5}}{D_{50}^{0.3}\left[\frac{(\rho s-\rho w)g}{\rho w \upsilon^2}\right]^{0.1}} \quad (3)$$

The sediment particle diameter is denoted by d, a is a reference level set equal to the roughness height. τ is the bed shear stress, and τ_c is the critical bed shear stress for movement of sediment particles according to Shield's curve. ρ_w and ρ_s are the density of water and sediment, υ is the viscosity of the water, and g is the acceleration of gravity (Olsen 1999, 2000, 2009).

2.2 *Initial Conditions*

Analysis was performed in clear water conditions. The diameter of the bed particles (d_{s50}) was 1.28 mm. The standard deviation (σ) of the bed particles was 1.3 mm. The discharge of flow was only from upstream (Q = 25 liter/second). The water depth in the channel upstream and the start of the straight run ($y_{initial}$) was equal to 11.6 cm. The Froude (Fr) number of the flow in the straight direction of the upstream of channel was 0.34. Channel walls were rigid and erosion took place only through the channel bed. The spur dike was T-shaped and 9 cm long, with an equal ratio of wing to web length. The dike was positioned at a 45-degree angle to the channel bend. Three relative curvatures related to the three sediment densities (ρ = 2.35, 2.5, and 2.65 g/cm^3) are analyzed in this study in nine cases. It took about eight hours to analyze each case for flow pattern and scour. The channel bend is shown as Fig. 1, in which Θ is the angle of each cross-section from the bend upstream.

2.3 *Boundary Conditions for Numerical Model*

SSIIM-1, Version 1 uses a structured grid. In a structured grid, there will always be one more grid line than grid cells in any given direction. Because boundary conditions are also needed, there will be a grid cell with zero thickness at the walls. Boundary conditions are required on all boundaries for the sediment flow calculation. The two most used types of boundary conditions are zero gradient and Dirichlet.

Zero gradient boundary conditions means the derivative of the variable at the boundary is zero. In other words, the value at the boundary is the same as the value in the cell closest to the boundary. This boundary condition is often used as the outflow boundary for the sediment concentration calculation and can also be used at walls. A zero gradient boundary condition is a type of Neumann boundary condition, while a Dirichlet boundary conditions means the values of a variable are given at the boundary. The gradient of all parameters in the outputs boundary are zero. In addition, the output rates of discharge must be introduced in the outgoing boundary conditions. The gradient of loss of the kinetic energy as well as the value of the kinetic energy at the water's surface is zero. The flux passing the bed and walls is zero. The discharge should be introduced in the bend entrance. The velocity gradient towards the wall is often very steep. If it is to be resolved in the grid, this will require too many grid cells. Instead, the wall laws area should be used. This means that it is assumed that the velocity profile follows a

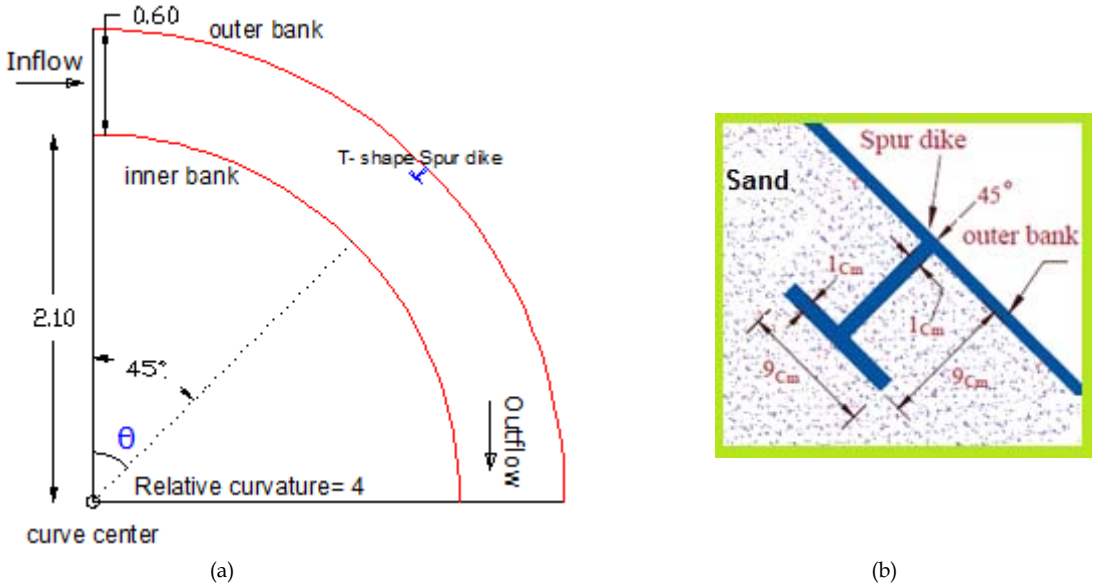

Figure 1. (a) Channel bed plan view and (b) magnified spur dike details.

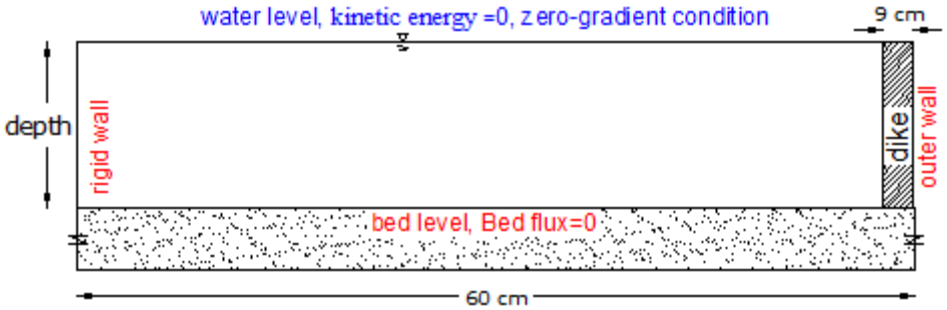

Figure 2. The boundary conditions at cross section.

certain empirical function,called a wall law. As Eqn. 4 shows, the wall law of Schlichting (1979) is used, where U is the velocity, U^* is the shear velocity, k is a constant coefficient equal to 0.4, y is the distance from the wall to the center of the cell, k_s is the roughness which is equal to 90% of the particles' diameter in the bed grading curve (Olsen 1999, 2000, 2001).

$$\frac{U}{U} = \frac{1}{K} Ln(30\, y / k_3) \qquad (4)$$

2.4 *Verification*

For verification of the model, SSIIM parameters were calibrated using laboratory model results. The intended experiments have been carried out in Tarbiat Modares University's hydraulics laboratory in Iran on a laboratory flume with a width of 60 cm and height of 70 cm in a compound straight and bent route (Fig. 3). The straight upstream route is 710 cm and is connected to a straight downstream route of 520 cm via a 90-degree bend, with an external radius of 270 cm and an internal radius of 210 cm. The spur dike used in this experiment is T-shaped. The length of the wing and web are nine cm with a height of 25 cm. This spur dike is vertical and non-submerged in a 45-degree position. Each experiment took the equivalent of 88% of the scour depth on experiment with an equilibrium time of 120 hours. This amount was 24 hours for each experiment (Vaghefi *et al*. 2012). Comparisons of the bed profiles in the cross sections at downstream and upstream of the spur dike are shown in Fig. 4. The model is capable of providing the bed topography. In other words, the SSIIM model could simulate the scour pattern in a 90-degree bend and is applicable in this study.

At a range of 0–10 cm from the outer bank, the bed profiles do not match with each other perfectly due to the presence of the spur dike in this area and the presence of the turbulent flow (Fig. 4). In the project's execution, the spur dike bed is protected from erosion by a collar layer; thus, the difference in the position of maximum scour is not significant. The difference in scour amounts in all sections appears in Table 1, where *de/ds* is the dimensionless

(a) (b)

Figure 3. The laboratory schematic model (a) before the test and (b) after the test.

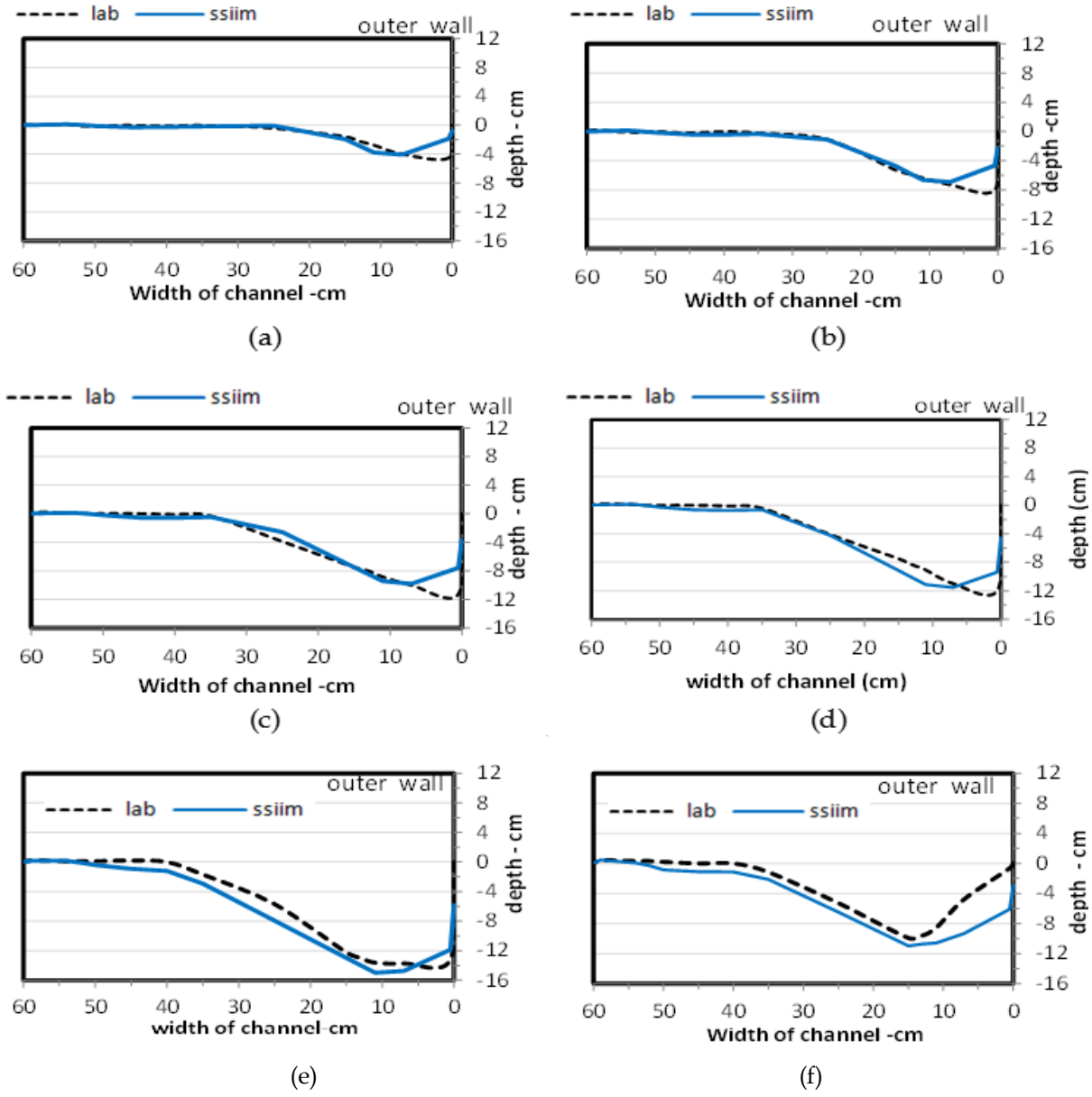

Figure 4. The bed profile in the cross sections of (a) 37.75^0 (b) 40^0 (c) 41.25^0 (d) 42^0 (e) 43.75^0 (f) 46.25^0.

Table 1. Difference in scour amounts related to the numerical and laboratory models.

Section 1	*de/ds*	Section	*de/ds*
Figure 4(a)	1.5%	Figure 4(d)	0.85%
Figure 4(b)	0.9%	Figure 4(e)	0.02%
Figure 4(c)	0.95%	Figure 4(f)	0.6%

parameter, and *de* is the difference in maximum scour amounts for the two models and *ds* is the maximum scour depth.

Figure 5 illustrates that the two models are a good match in terms of the quantity and range of maximum scour so that the maximum scour occurs in the dike upstream near the tip of its wing. In comparison, results are in good agreement.

Figure 5 illustrates that *Rc* is the curvature radius of the bend. *X* and *Y* are the distance of the coordinates from the center of curve. To show the amount of bed changes, the dimensionless quantity (ds/y) is used which represents the ratio of the change in the bed depth to the initial water depth ($y_{initial}$ = 11.6 cm).

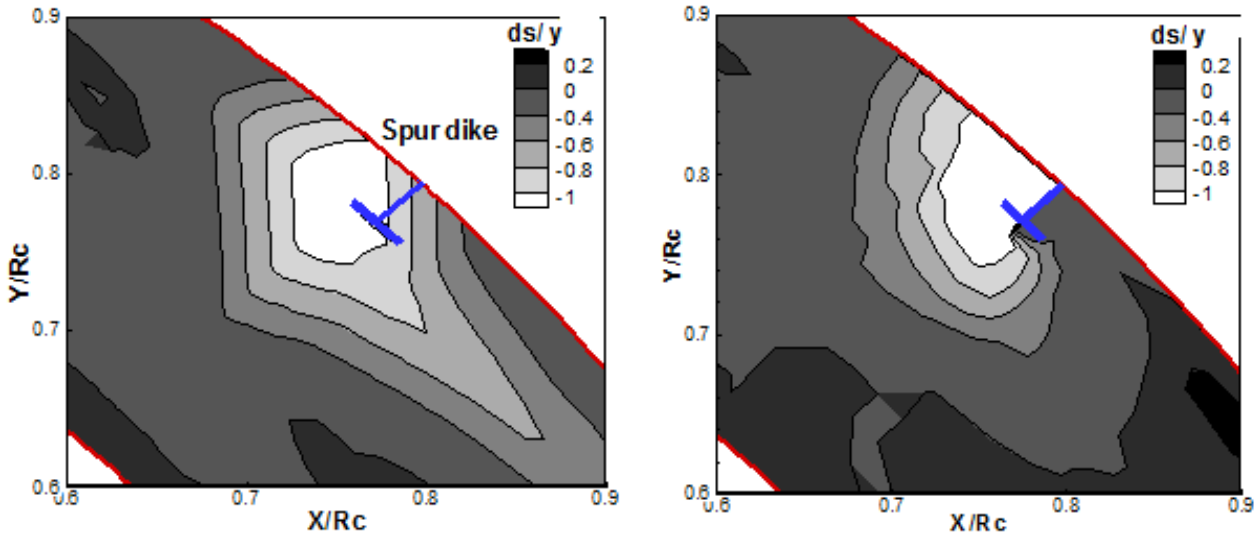

Figure 5. Bed changes around in the spur dike (a) numerical data and (b) laboratory findings.

3. Results and Discussion

To analyze the effect of the bed sediment density on bed changes, the current researchers modeled a 90-degree bend channel with three relative curvatures, with *R/B* = 2, 3, and 4, where *R* is the radius of curvature and *B* is the width of channel. Sediment density (ρ) with respect to the empirical values and based on the gender of the river sediments were set at 2.35, 2.5, and 2.65 g/cm^3. According to Figs. 6–8, in all relative curvatures (*R/B*), the bed topography varies by increasing the sediment density, but the maximum amount of scour always occurs near the head of dike wing at the dike upstream, and the maximum amount of sedimentation occurs at the inner bank of bend exit. The laboratory study of Vaghefi *et al.* (2012) showed in this case that *R/B* = 4.

As the Figs. 6 and 7 illustrate, the bed sediments were moved to the channel downstream from around the spur dike. By increasing the sediment densities from 2.35 to 2.65, the maximum amounts of scour and sedimentation were reduced (Table 2).

In a channel bend with a relative curvature equal to 3 and 4, the second scour hole is formed at the inner bank of the bend exit; however, when *R/B* = 2, this hole is not formed because the bend length is less than when *R/B* = 3 and 4. When *R/B* = 2, the bend downstream is affected by the main scour hole which is formed at the upstream of the dike wing). This influence continues until the bend exit.

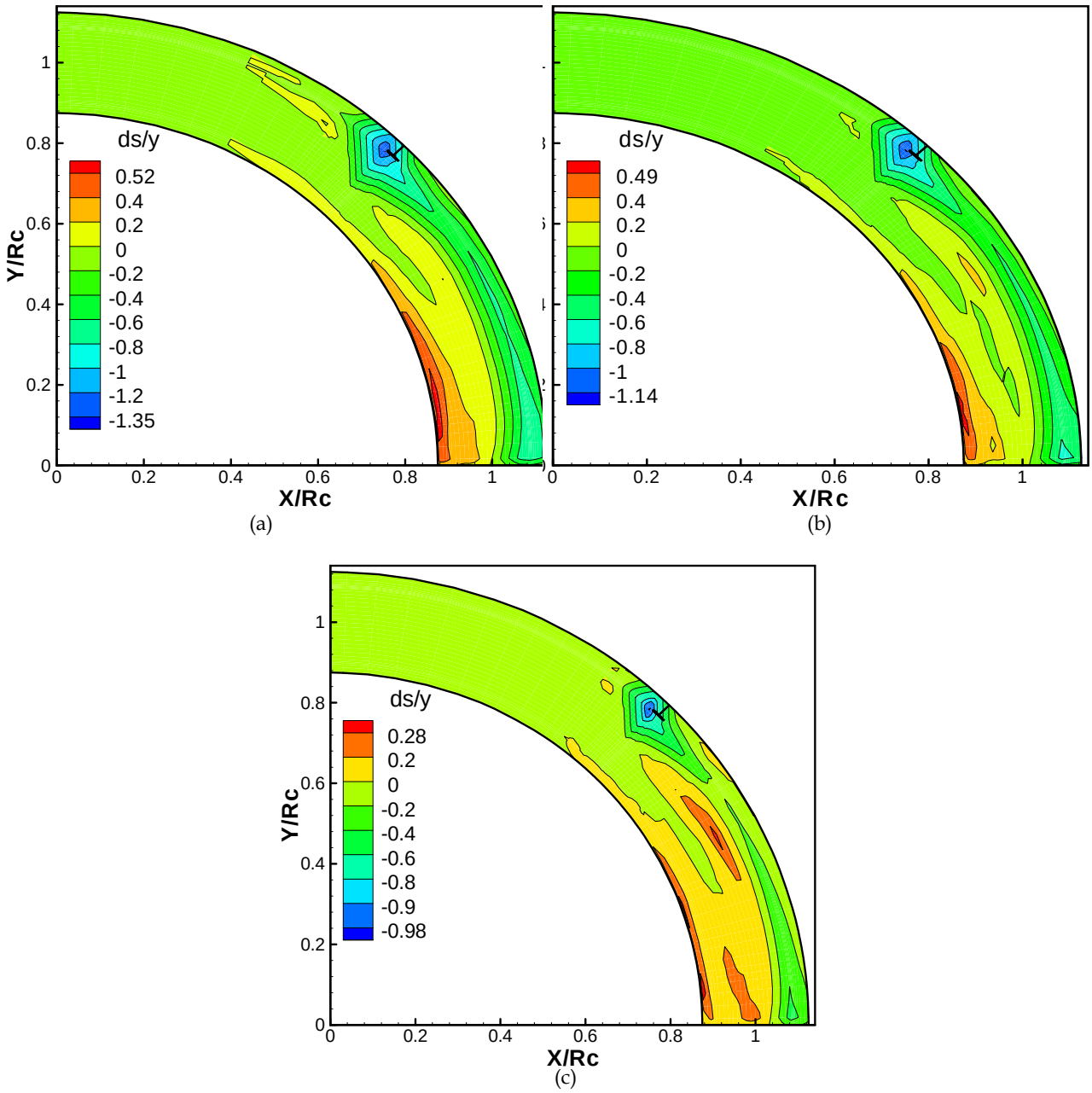

Figure 6. Bed topography when R/B = 4 (a) ρ = 2.35 (b) ρ = 2.5 (c) ρ = 2.65.

Table 2. Redacting the maximum scour and sedimentation due to an increase in density.

Relative curvature	Reading the scour	Redacting the sedimentation
R/B = 2	25.98	10%
R/B = 3	25.93%	23.91%
R/B = 4	27.41%	46.15

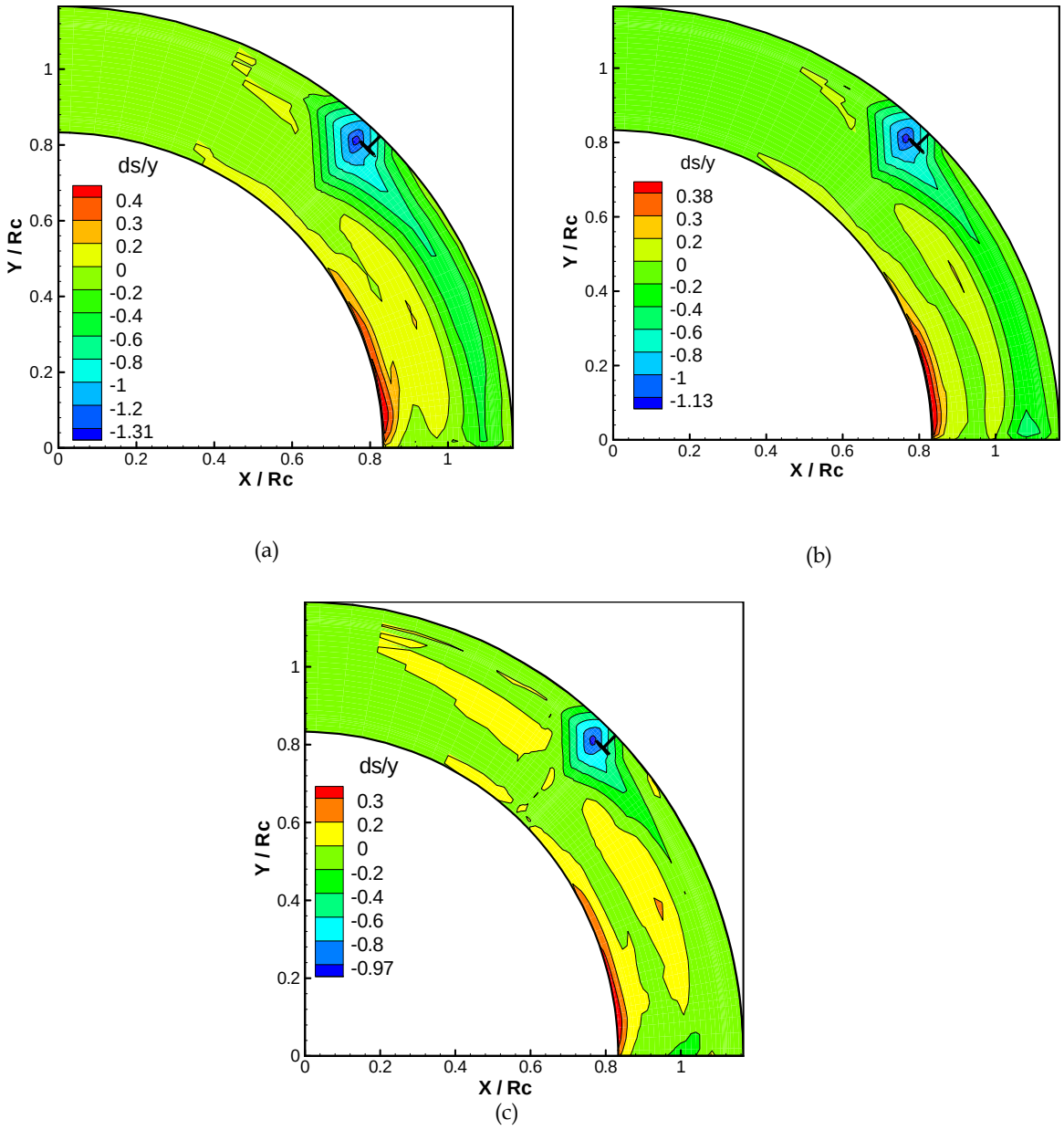

Figure 7. Bed topography when *R/B* = 3 (a) ρ = 2.35 (b) ρ = 2.5 (c) ρ = 2.65.

As Figs. 6–8 illustrate, for *R/B* =4 with an increases in sediment density, at the dike upstream the range of sedimentation decreases. This sedimentation was created by transferring a portion of the sediment from the spur dike bed due to the longitudinal vortices. Also, downstream of the spur dike and at an angle of about $\Theta = 60^0$, a sedimentary bar expands in the middle of the channel width, such as when the density equals 2.65. It has the highest quantity. Vaghefi *et al.* (2015), by investigating the changes in bed topography in different relative curvatures concluded that when ρ = 2.35, by increasing the relative curvature, the maximum amount of scour increases in the dike upstream. In this paper, it can be seen that when ρ = 2.5 and 2.65 g/cm^3, by increasing the relative curvature according to Table 3, the maximum amount of scour increased as expected.

As Figs. 9 and 10 show, the maximum amounts of scour and sedimentation are reduced because, by increasing the sediment density, the mass of the Sediment increases; therefore, more force is needed to pick up and move the sediment. Since the conditions are the same for all analyses, the

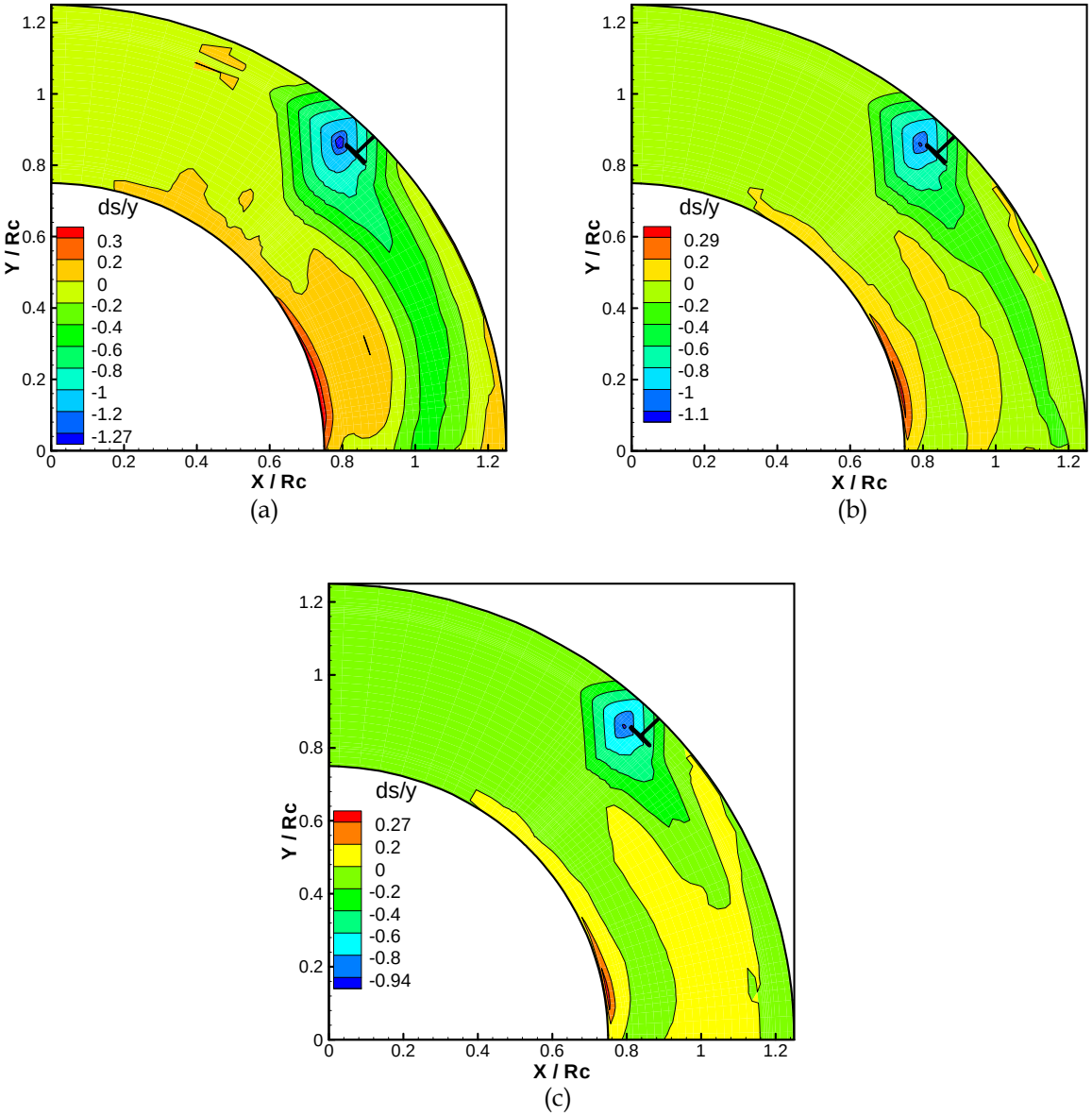

Figure 8. The bed topography when *R/B* = 2 (a) ρ = 2.35 (b) ρ = 2.5 (c) ρ = 2.65.

Table 3. The dimensionless of maximum scour due to increase in density and relative curvature.

Sediment density g/cm³	***R/B* = 2**	***R/B* = 3**	***R/B* = 4**
P = 2.35 (Results of Vaghefi *et al.* (2015))	*ds/y* = -1.27	*ds/y* = -1.31	*ds/y* = -1.35
P = 2.5 (Results of this study)	*ds/y* = -1.10	*ds/y* = -1.13	*ds/y* = -1.14
P = 2.65 (Results of this study)	*ds/y* = -0.94	*ds/y* = -0.97	*ds/y* = -0.98

maximum scour decreases. By reducing the amount of scour, less sediment is transported at the bend downstream and the amount of maximum sedimentation is reduced.

By increasing the relative curvature of the bend, based on change in sediment density, the trend of change in the scour amount increases (Fig. 10) and the greater change of the diagram slope is evident when *R/B* = 4.

4. Conclusion

The effect of sediment density (ρ = 2.35, 2.5, and 2.65 g/cm³) on the bed topography of the channel with three relative curvatures (*R/B* = 2, 3, and 4) illustrates nine cases of installing the T-shaped spur dike in the middle of the outer bank (three relative curvatures related to the three sediment densities). The following results were obtained:

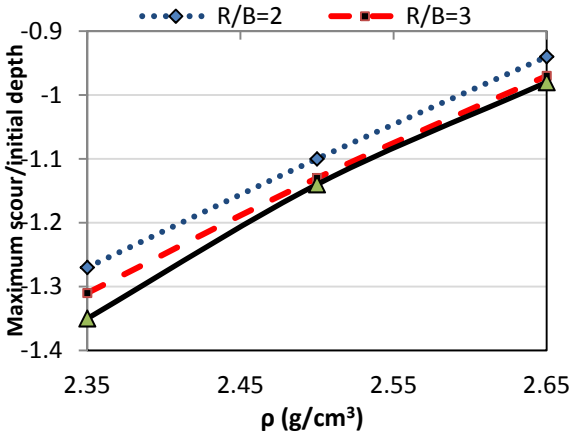

Figure 9. Diagram of the maximum scour based on relative curvature and density.

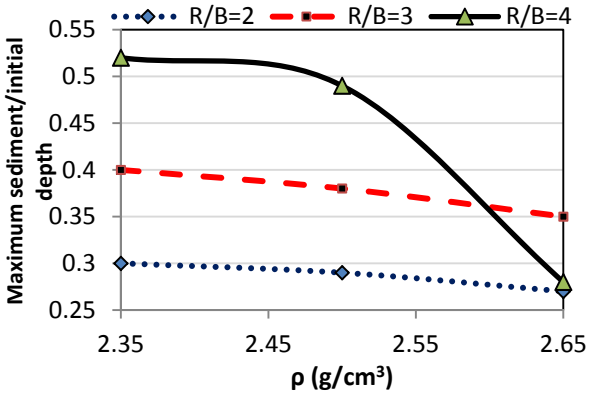

Figure 10. Diagram of the maximum sedimentation based on relative curvature and density.

1. In all cases, the maximum amount of scour occurred near the head of the dike wing at the dike upstream, and the maximum amount of sedimentation occurred at inner bank of the bend exit.

2. In a channel bend with a relative curvature equal to 3 and 4, the second scour hole was formed at the inner bank of the bend exit.

3. When *R/B* = 4 by increasing the sediment density, at the dike upstream, the range of the amount of the sedimentation decreased.

4. By increasing the sediment density from 2.35 to 2.65 (gram/cm^3) when *R/B* = 4, the maximum amounts of scour and sedimentation decreased to 27.41% and 46.15%, respectively. When *R/B* = 3, the maximum amounts of scour and sedimentation decreased to 25.93% and 23.91%, respectively. When *R/B* = 2, the maximum amounts of scour and sedimentation decreased to 25.98% and 10%, respectively.

References

Abhari M, Ghodsian M, Vaghefi M, Panahpur N (2010), Experimental and numerical simulation of flow in a 90 degree of bend. *Flow Measurement and Instrumentation* 21: 292–298

Azinfar H (2010), Flow resistance and associated backwater effect due to spur dikes in open channels. A thesis submitted to for the degree of Doctor of Philosophy, Department of Civil and Geological Engineering, University of Saskatchewan Saskatoon, Canada.

Booij R (2002) Modeling of the secondary flow structure in river bends. In, River Flow, Bousmar and Zech (Eds), ISBN 90 5809 509 6: 127:133.

Da Silva AMF, Yalin MS (1997), Laboratory measurements in sine-generated meandering channels. *International Journal of Sediment Research* 12(1): 16–28.

Elawady E, Michiue M, Hinokidani O (2001), Movable bed scour around submerged spur-dikes. *Annual Journal of Hydraulic Engineering* 45: 373–378.

Ghodsian M, Vaghefi M (2009), Experimental study on scour and flow field in a scour hole around a T-shape spur dike in a 90° bend. *International Journal of Sediment Research* 24: 145–158.

Gill MA (1972) Erosion of sand beds around spur dikes. *Journal of the Hydraulics Division* 98(9): 91–98.

Hua L, Roger A, Kuhnle B, Barkdoll D (2006), Countermeasures against scour at abutments. Research Report No.49, Channel and Watershed Processes Research Unit, National Sedimentation Laboratory, USDA Agricultural Research Service Oxford.

Lian HC, Hsied TY, Yang JC (1999), Bend-flow simulation using 2d depth–averaged mode. *Journal of Hydraulic Engineering* 125(10): 1097–1108.

Nouh MA, Townsend RD (1979), Shear-stress distribution in stable channel bends. *Journal of the Hydraulics Division, American Society of Civil Engineers* 105 (HY10) Proceedings Paper 14898, 1233–1245.

Olsen NRB (1999), Computational fluid dynamics in hydraulic and sedimentation engineering. Department of Hydraulic and environmental Engineering, Norwegian University of Science and Technology, Class notes, Revision 2nd.

Olsen NRB (2000), CFD algorithms for hydraulic engineering. Class notes, Department of Hydraulic and environmental Engineering, Norwegian University of Science and Technology, Norway.

Olsen NRB (2001) CFD modeling for hydraulic structures. Norwegian University of Science and Technology, Preliminary 1st edition, 8 May. ISBN 82-7598-048-8.

Olsen NRB (2009), A three-dimensional numerical model for simulation of sediment movement in water intakes with multi-block option. Department of Hydraulic and Environmental Engineering, Norwegian University of Science and Technology, SSIIM User's Manual.

Sclafani P, Thornton CI, Cox AL, Abt SR (2012), Methodology for predicting maximum velocity and shear stress in a sinuous channel with bend way weirs using 1-D HEC-RAS modeling results. Colorado State University, Engineering Research Center

Shukry A (1949), Flow around bends in an open flume. *American Society of Civil Engineers*, No. 2411, 115(1): 785-789.

Schlichting H (1979), Boundary-layer theory. New York: McGraw-Hill.

Vaghefi M, Ghodsian M, Salehi Neyshabouri SAA (2012), Experimental study on scour around a T-shaped spur dike in a channel bend. *Journal of Hydraulic Engineering* 138(5): 471–474.

Vaghefi M, Safarpoor Y, Hashemi SS (2014), Effect of T-shape spur dike submergence ratio on the water surface profile in 90 degree channel bends with SSIIM numerical model. *International Journal of Advanced Engineering Applications* 7(4): 1–6.

Vaghefi M, Safarpoor Y, Hashemi SS (2015), Effects of relative curvature on the scour pattern in a 90° bend with a T-shaped spur dike using a numerical method. *International Journal of River Basin Management* 13(4): 501-514.

Van Rijn L (2007), Unified view of sediment transport by currents and waves. II: Suspended Transport. *Journal of Hydraulic Engineering* 133(6): 668–689.